Italian Journal of Engineering Geology and Environment
www.ijege.uniroma1.it

REMOTE SENSING TECHNOLOGIES SUPPORTING ROCKFALL HAZARD ASSESSMENT FOR TRANSPORTATION ROUTES MANAGEMENT

Giandomenico MASTRANTONI[(*)], Antonio COSENTINO[(*, **)], Marta ZOCCHI[(*)], Jagadish KUNDU[(***)], Angelo DANDINI[(****)], Maurizio MARTINO[(****)], Alfredo MONTAGNA[(****)], Gabriele SCARASCIA MUGNOZZA[(*)] & Paolo MAZZANTI[(*, **)]

[(*)]Sapienza University of Rome - Department of Earth Sciences and CERI Research Centre - Rome, Italy
[(**)]IntelligEarth S.r.l., Start-up of Sapienza University of Rome - Rome, Italy
[(***)]Institute of Geological and Nuclear Sciences - GNS Science - Avalon, Lower Hutt, New Zealand
[(****)]ANAS S.p.A. - Direzione Tecnica - Roma, Italy.
Corresponding author: giandomenico.mastrantoni@uniroma1.it

EXTENDED ABSTRACT

Le tecnologie di telerilevamento possono rappresentare uno strumento fondamentale per la valutazione e la gestione del rischio da frana lungo le reti di trasporto. Questo studio esamina l'applicazione della fotogrammetria aerea da drone e del laser scanner terrestre per la caratterizzazione geostrutturale e geomeccanica degli ammassi rocciosi, nonché il potenziale delle tecniche di fotomonitoraggio per l'identificazione di cambiamenti legati a processi di instabilità gravitativa di versante. L'area di studio coinvolge il versante in roccia che delimita i centri abitati di Maiori e Minori (Salerno, Italia), il quale mostra evidenze di fenomeni franosi passati ed attualmente attivo per crolli in roccia.

I rilievi fotogrammetrici sono stati condotti utilizzando due piattaforme aeree: un DJI Mavic 3 equipaggiato con sensore ottico fisso e un DJI Matrice 200 dotato di fotocamera Zenmuse X5S con stabilizzatore triassiale Gimbal. Per investigare l'effetto della distanza di acquisizione delle immagini sulle proprietà delle nuvole di punti risultanti, i voli sono stati effettuati a due distanze differenti (15 e 35 metri) su una porzione selezionata della parete rocciosa. Questo approccio ha permesso di generare quattro nuvole di punti a differente risoluzione, consentendo un'analisi comparativa dell'efficacia delle diverse configurazioni sensore-distanza per l'estrazione delle discontinuità. Il rilievo TLS è stato eseguito utilizzando un RIEGL VZ-1000, con acquisizioni da due postazioni differenti per ridurre le zone d'ombra.

Le nuvole di punti derivate sono state analizzate per estrarre parametri geostrutturali e geomeccanici, tra cui l'orientazione delle discontinuità e le loro spaziature, nonché per definire la qualità dell'ammasso roccioso. Le analisi semi-automatiche hanno dimostrato la validità di entrambi gli approcci di rilievo, sebbene la presenza di reti paramassi abbia introdotto sfide significative nella ricostruzione fotogrammetrica. In particolare, è stato osservato che le nuvole di punti fotogrammetriche possono presentare approssimazioni topografiche rispetto alle nuvole LiDAR, ma garantiscono una copertura più completa dello scenario investigato grazie all'uso di sistemi aerei a pilotaggio remoto.

Indipendentemente dalla tecnologia di acquisizione, il rilievo geostrutturale semi-automatico su nuvole di punti 3D rende possibile analizzare tutta l'area in esame in maniera oggettiva e ripetibile, rendendolo preferibile al rilievo manuale di campagna, ma deve essere sempre guidato e validato da dati di sito. A tale riguardo, la caratterizzazione dell'ammasso roccioso è stata supportata da misure dirette delle discontinuità e dei parametri geomeccanici quali il valore di rimbalzo del martello Schmidt, il calcolo volumetrico dei giunti (Jv), il valore RQD, e le loro condizioni (persistenza, apertura, riempimento, rugosità e alterazione).

Lo studio ha inoltre esplorato l'utilizzo del fotomonitoraggio per il rilevamento dei cambiamenti (Change Detection). Questa tecnica si è dimostrata particolarmente efficace sfruttando le ortofoto generate tramite il rilievo fotogrammetrico aereo.

Questo lavoro dimostra come l'integrazione di diverse metodologie di telerilevamento, combinate con validazioni di campo, fornisca un quadro robusto e affidabile per la valutazione della stabilità dei versanti in roccia, contribuendo significativamente alla gestione del rischio delle infrastrutture di trasporto, particolarmente in contesti geologici complessi dove i metodi di rilievo tradizionali risultano limitati o impraticabili.

IJEGE, 2 (2024): 17-33, DOI: 10.4408/IJEGE.2024-02.O-03
E-ISSN 2035-5688 | ISSN 1825-6635 / ©Author(s)

ABSTRACT

Remote sensing technologies offer enhanced capabilities for the assessment of rockfall hazard impacting transportation networks and the related risk management. This study examines the application of UAV-based photogrammetry and terrestrial laser scanning (TLS) for comprehensive geomechanical characterisation of rock masses, as well as the potential of photomonitoring techniques for slope stability assessment. A rock cliff located between the towns of Minori and Maiori (SA, Italy) was selected as the test site.

Photogrammetric surveys were conducted using DJI Mavic 3 and DJI Matrice 200 aerial platforms. The surveys were performed at two flight distances (15 and 35 meters) for a portion of the rock face to investigate the effect of camera-to-subject range on the resulting point cloud properties. The derived point clouds were analysed to extract geostructural and geomechanical parameters, including discontinuity orientation, normal spacing, Jv, RQD, and block volumes. Semi-automatic analyses demonstrated the viability of both photogrammetric and TLS approaches, while highlighting the need for methodological adaptations in the photogrammetric method due to reconstruction challenges posed by the installed protective rockfall net.

Additionally, the study explored the use of photomonitoring for change detection of natural slopes, highlighting its potential as a complementary technique. The integration of multiple remote sensing methods provides a robust framework for slope stability assessment and management, contributing to enhanced transportation infrastructure resilience.

Keywords: *terrestrial laser scanning, drone photogrammetry, photomonitoring, rock mass characterization, rock slope stability, transportation infrastructure*

INTRODUCTION

The characterization and monitoring of unstable rock faces using traditional geomechanical methods and remote sensing techniques are of paramount importance for the protection of infrastructures and human life. To comprehend the evolutionary processes of these geological features, it is essential to acquire detailed information on rock mass properties. Accurate characterisation of discontinuity properties is a fundamental step in predicting the mechanical behaviour of rock masses (Barton, 2013; Barton & Choubey, 1977; Goodman, 1991). Parameters such as orientation, spacing, and persistence are crucial for estimating block shape and dimensions, as well as identifying areas prone to instability (Francioni *et alii*, 2020; Gigli & Casagli, 2011; Guzzetti *et alii*, 2004). Manual field surveying has traditionally been the standard approach for geomechanical analysis of rock masses. However, this method can be expensive and inadequate for the whole extent of the study area, or even impossible to execute due to site inaccessibility, safety conditions, and considerable rock face heights (Coggan *et alii*, 2007). Modern remote sensing techniques, such as photogrammetry and LiDAR, have emerged as valuable tools for rock mass characterisation. These technologies provide high-resolution models of rock faces in the form of point clouds, enabling manual, semi-automatic, and automatic 3D structural evaluations of rock masses (Gallo *et alii*, 2021; Kundu *et alii*, 2024; Mazzanti *et alii*, 2017, 2015; Peralta *et alii*, 2024; Robiati *et alii*, 2023, 2019).

PhotomonitoringTM represents a novel monitoring solution that leverages the wide availability of sensors across multiple platforms, including aircraft, drones, and satellites (Cosentino *et alii*, 2024; Mazza *et alii*, 2023; Mazzanti *et alii*, 2020). These sensors acquire optical or multispectral data to obtain information on territorial changes or ground element displacements through the application of appropriate Digital Image Processing algorithms. This technique operates across various temporal and spatial scales, making it an ideal tool for investigating and monitoring diverse processes affecting territories, environments, and their interactions with infrastructure. The analysis algorithms primarily rely on two distinct techniques: Digital Image Correlation (DIC) for studying and quantifying the displacement of elements of interest and Change Detection (CD) for quantifying changes (Guerriero *et alii*, 2020; Mazzanti *et alii*, 2020).

This study focuses on the application of UAV-based photogrammetry and Terrestrial Laser Scanning (TLS) for the geostructural and geomechanical characterisation of rock masses supporting rockfall hazard analysis. Moreover, we investigated the influence of the data acquisition technology (*i.e.*, photogrammetry vs laser scanning), as well as the influence of the type of drone on the resulting point cloud, thus exploring their performance and limits. Specifically, we examined the effects on the point clouds and the derived discontinuities caused by the camera type (*i.e.*, image resolution) and the capture distance. Finally, this study presents an application of the photomonitoring technique for rockfall detection from orthomosaics images.

CASE STUDY

The study area is located between the towns of Maiori and Minori (Figure 1) along the eastern coast of the Sorrento Peninsula (Southern Italy). The area has a considerable extent along the coastline, with a topography defined by the abrupt transition from the coastal zone to the mountainous hinterland of the peninsula, with peaks reaching over 1,000 m in height. The coastline, dominated by these high, structurally controlled cliffs that plunge directly into the Tyrrhenian Sea, is interrupted only by the narrow, stream-fed beaches at the valley mouths.

From a geological perspective, the Sorrento Peninsula is a

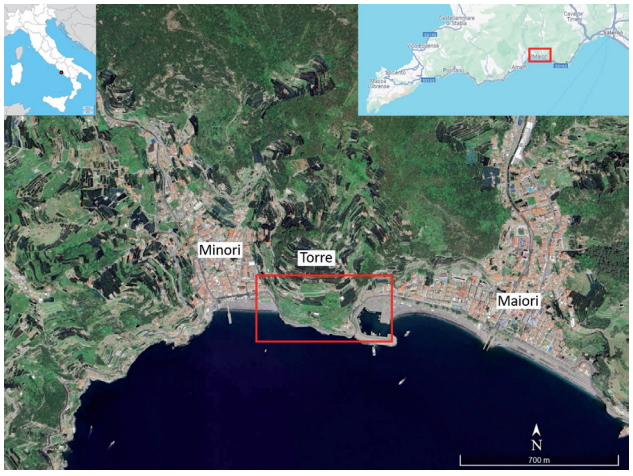

Fig. 1 - The study area (identified within the red rectangle) is located along the Amalfi Coast, between the towns of Maiori and Minori

segment of the Southern Apennine fold and thrust belt. It results from the Neogene deformation that involved the oceanic and continental margin domains of the Apulian margin (Patacca & Scandone, 2007; Zappaterra, 1994). The deformed Mesozoic carbonate succession presently exposed in the Peninsula constitutes the ENE-WSW elongated Lattari Mountains ridge. This structural high is mainly composed of Upper Triassic to Upper Cretaceous shallow-water limestones and dolostones, unconformably overlaid by Miocene foredeep wedge-top basin siliciclastic deposits (*e.g.*, sandstones, calcareous sandstones, and conglomerates). Eventually, Quaternary pyroclastic rocks locally cap the whole sedimentary pile (Carannante *et alii*, 2000; Iannace *et alii*, 2011; Tavani *et alii*, 2013; Vinci *et alii*, 2017). The study area is located in the southeastern sector of the peninsula and is characterized by the widespread presence of the carbonate and dolostone deposits of the Monti Lattari tectonic unit, interspersed with limited exposures, mainly in correspondence with the valley incisions, of Quaternary deposits belonging to the Sele Plain–Gulf of Salerno Basin (Iannace *et alii*, 2015). As depicted in Figure 2, the geological setting of the study area is dominated by the Triassic-Jurassic carbonate-dolostone successions, with limited occurrences of younger Pliocene-Holocene alluvial (*i.e.*, Sintema di Amalfi) and beach sediments, as well as Pleistocene-Holocene volcaniclastic deposits (consisting of loose pyroclastic materials often reworked by slope processes) in the northern portions. The contacts between these lithological units are primarily controlled by tectonic elements, except for the alluvial cover materials infilling the valleys carved into the Mesozoic bedrock (Iannace *et alii*, 2015).

The Maiori side promontory is entirely composed of dolomites and chert-bearing limestones dipping towards SSW, exhibiting variable structural-stratigraphic settings from east to west. The rock mass in the eastern portion of the

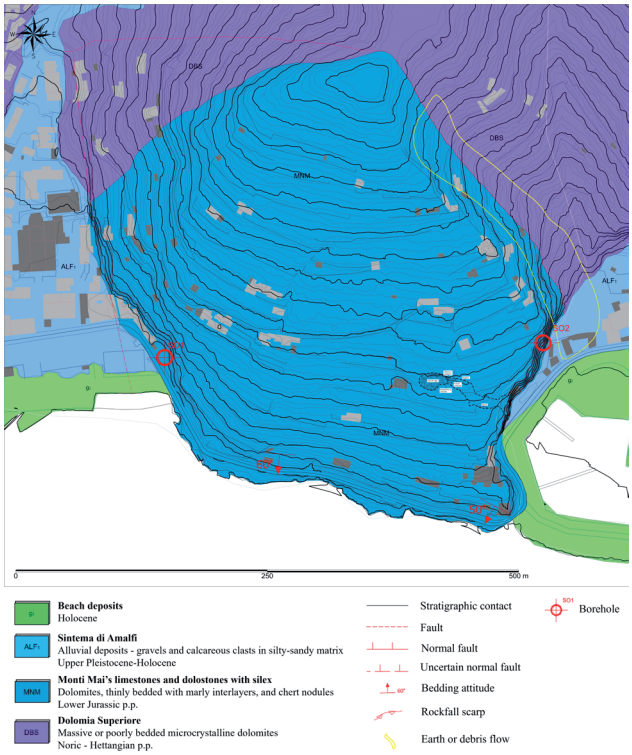

Fig. 2 - Geological map of the study area derived by ANAS through technical field surveys

promontory appears massive or poorly bedded, interbedded with thick marly limestone layers, and is affected by multiple tectonic discontinuities, which contributes to the chaotic and disarticulated structure of the rock mass. Moving westward across the promontory (Minori side), the chaotic structure gradually changes into more distinct bedding and a less pervasive deformation pattern. The dolomitic-carbonate succession is organized in thin beds (centimetric to decimetric) dipping towards SSW, which progressively thicken upwards in the stratigraphic sequence.

The geological and geomorphological setting of the study area, dominated by high vertical cliffs along the eastern and western boundaries and intersected by numerous tectonic discontinuities, results in significant rockfall and toppling hazard conditions, which is particularly concerning given that this route serves as the sole vehicular connection between the two settlements and Amalfi town. The elevated exposure to geohazards, combined with the current challenges of traffic management along the S.S. 163 (single-lane traffic controlled by traffic lights), led ANAS to further investigate the geological context, with reference to the geostructural survey of the two rocky slopes insisting on the road infrastructure (Figure 2), thus identifying the optimal design solutions aimed at mitigating the risk of rockfalls in this section of the Amalfi Coast.

MATERIALS & METHODS

In this section, the data and methods of the study are presented. Figure 3 shows the adopted workflow, which takes in input the data generated from terrestrial laser scanning (TLS) and aerial photogrammetry. The point clouds and the orthomosaics were computed for both the Minori and Maiori side of the rock cliff. Conversely, the geostructural and geomechanical analysis, as well as the influence of drone type and camera-to-subject distance on the results was carried out for the Minori side only.

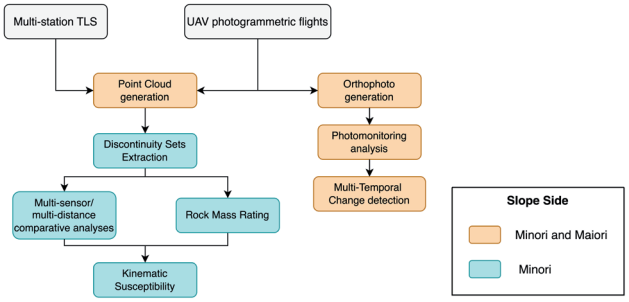

Fig. 3 - Workflow for data acquisition and processing implemented in the present study

Aerial Photogrammetry

Photogrammetric surveys of the rock cliffs in Minori and Maiori were conducted on February 28 and June 7, 2023, utilising two Unmanned Aerial Systems (UAV): a DJI Mavic 3 equipped with a fixed optical sensor, and a DJI Matrice 200 outfitted with a Zenmuse X5S camera and a three-axis Gimbal stabiliser (Figure 4). The sensor specifications are provided in Table 1. The optical images were subsequently processed using structure-from-motion algorithms (James & Robson, 2012; Luhmann *et alii*, 2019; Seitz *et alii*, 2006; Spetsakis & Aloimonos, 1990), yielding both point clouds and 3D surface model of the rock faces. During the surveys, a series of points along the road trajectory were sampled using a GNSS station to georeference the point clouds within an international coordinate system. Due to the complex terrain, it was not feasible to install known markers along the rock face. The accurate and uniform placement of markers in space and elevation within the survey area is crucial for achieving proper georeferencing and minimising distortions induced by photogrammetric processing (Carrivick *et alii*, 2016). In photogrammetry, the digital camera's

Fig. 4 - Unmanned aerial systems used for photogrammetric surveys of the rock cliffs in Minori and Maiori

	DJI Mavic 3	DJI Matrice 200
Sensor	4/3" CMOS, 20 MP	4/3" CMOS, 20.8 MP
FOV [°]	84	72
Image size [px]	5280×3956	5280×3956

Tab. 1 - Specifications of the optical sensors mounted on the drones used to perform the photogrammetric surveys

characteristics and the image acquisition distance can significantly impact the resulting product (Sapirstein, 2016). Flights were conducted at two different capture distances (15 and 35 metres) only for a limited portion of the Minori rock cliff, thus investigating the effect of object distance on the properties of the derived point cloud. This approach yielded four point clouds with varying resolutions, resulting in six different point clouds.

Terrestrial laser scanning

The LiDAR survey of the rock cliffs in Minori and Maiori was conducted using a RIEGL VZ-1000 Terrestrial Laser Scanner (TLS) (Figure 5). Two scanning positions were strategically selected for each rock cliff to provide diverse capture angles and minimise shadowing effects and occlusions (Abellán *et alii*, 2014; Farmakis *et alii*, 2020). Subsequently, the point clouds from each rock cliff were merged to obtain a single, comprehensive virtual outcrop model. In addition to recording the laser signal amplitude, each point in the cloud was attributed with real colour information in RGB format. This colourization was achieved through photographs captured by the camera integrated into the TLS system. This approach enhanced the visual and qualitative properties of the resulting point cloud, facilitating a more detailed analysis and interpretation of the rock face characteristics.

Fig. 5 - Specifications of the optical sensors mounted on the drones used to perform the photogrammetric surveys

Rock mass characterisation

A comprehensive geomechanical field survey was conducted involving direct physical measurements, to characterise the rock mass in the Minori side of the rock slope. However, data collection was significantly hindered by the presence of wire mesh covering large portions of the slope, which impeded or precluded the direct measurement of geomechanical parameters in outcrops along the road. The survey focused on gathering data about the orientation and inclination of discontinuities, as well as overall rock mass quality (Ferrero *et alii*, 2009). A total of 45 discontinuities were measured across two distinct stations on the Minori slope. These stations also served as sites for collecting geomechanical data, including volumetric joint count (Jv), discontinuity spacing, groundwater conditions (GW), and discontinuity conditions, encompassing: *i*) persistence (in metres), *ii*) aperture (in millimetres), *iii*) infilling (in millimetres), and *iv*) weathering conditions. The volumetric joint count (Jv) is defined as the number of joints encountered in one cubic metre of fractured rock mass. It quantifies the number of intersecting discontinuities within the fractured rock mass per cubic metre (Palmstrom, 2005). The RQD value was indirectly calculated from the Jv using the correlation proposed by (Palmstrom, 2005). This approach to data collection allowed for a restricted characterization of the rock mass due to the physical limitations posed by site conditions.

In addition to manual field measurements, remote geostructural analyses were conducted using the photogrammetric point clouds derived from images captured by the drone DJI Matrice 200. Leveraging the georeferenced point clouds and the virtual compass feature within the Cloud Compare analysis and management software (Girardeau-Montaut, 2006), a total of 150 evenly distributed discontinuity orientations were extracted along the entire central portion of the rock cliff. This remote sensing approach significantly expanded the dataset beyond what was achievable through traditional field methods. The point clouds georeferencing ensured spatial accuracy, while the virtual compass tool facilitated quick and reliable orientation measurements without the need for physical access to the rock face. These remotely collected measurements serve a dual purpose: *i*) they form a comprehensive reference dataset that encompasses a larger area of the rock face than was accessible for manual measurements; *ii*) this dataset will be used to guide and validate semi-automatic analyses, providing a robust foundation for further geostructural assessments. The integration of field-based and remote sensing techniques allows for a more thorough and spatially extensive characterization of the rock mass, enhancing the overall understanding of the site's geomechanical conditions.

The semi-automatic geostructural characterization of the Minori side of the rock slope was performed using the Discontinuity Set Extractor (DSE) software, which employs a semi-automatic approach for identifying and extracting planar surfaces from 3D LiDAR or photogrammetric point clouds in rock slopes (Riquelme *et alii*, 2014). This method appropriately clusters individual points into families that define the principal orientations and, consequently, the discontinuity systems (Riquelme *et alii*, 2017). For analysis purposes, the Minori point cloud was subdivided into two distinct areas (A1 and A2) (Figure 6). The A1 zone corresponds

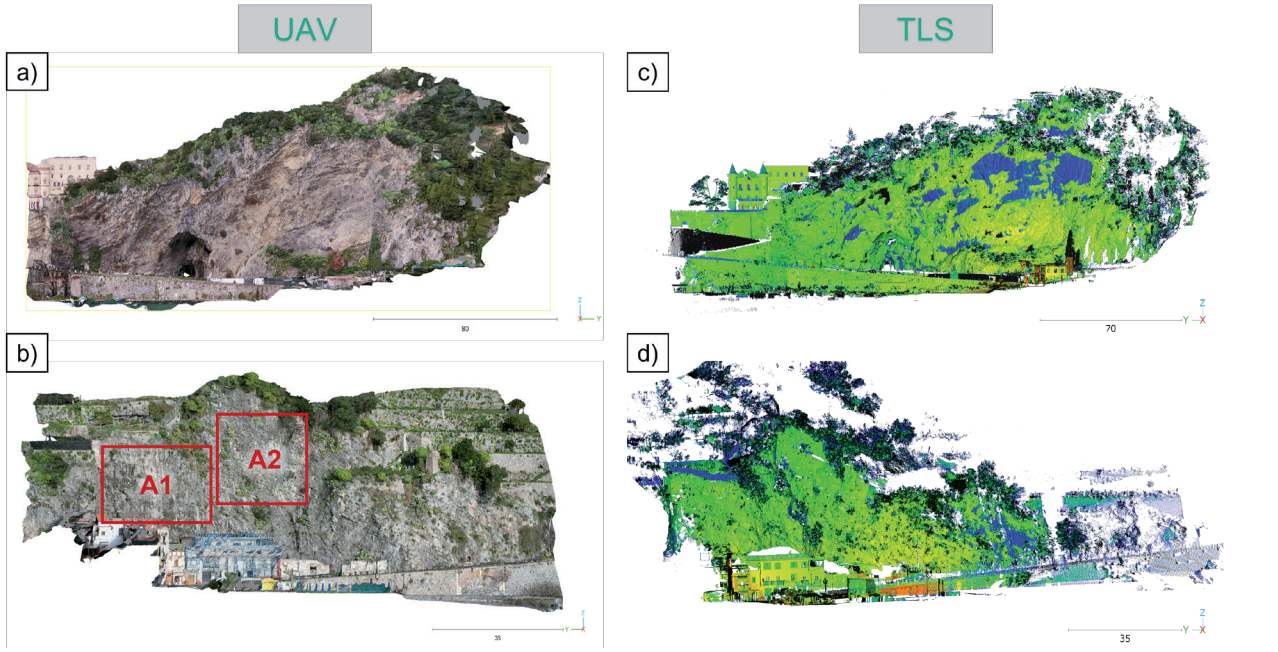

Fig. 6 - Overview of 3D point clouds related to the rock cliffs at Maiori (a, c) and Minori (b, d) locations. The boxes plotted in red show areas A1 and A2 selected for semi-automatic remote geostructural analysis

to the western slope, where there is a continuous presence of protective containment nets in contact with the rock mass, which could potentially influence the geostructural analysis. In contrast, Area A2 is devoid of such nets and is located in the central part of the slope. Both areas exhibit low to medium-height vegetation, which was filtered out before the analyses. To assess the impact of protective structures on the analysis results, a comparative study was conducted: *i*) results derived from the photogrammetric point clouds (including the protective nets) were compared with those obtained from LiDAR point clouds; *ii*) the LiDAR data allowed for the accurate removal of the protective nets from the point cloud. This selective removal was facilitated by the distinct laser signal amplitude values associated with the nets, which significantly differed from the amplitude range characteristic of the rock mass (Figure 6c, d) (Abellán *et alii*, 2014; Jaboyedoff *et alii*, 2018). This comparative approach enables a quantitative evaluation of the protective structures influence on semi-automatic geostructural analysis. By comparing results from datasets with and without the protective nets, it becomes possible to isolate their effect and ensure the accuracy of the rock mass characterization.

Rockfall susceptibility analysis

- *Rock Mass Rating*

Normal joint spacing, defined as the perpendicular distance between two joints within a joint set, is a critical parameter in assessing rock mass structure (Kim *et alii*, 2007). The presence of joints inherently reduces rock mass strength, with joint spacing regulating the degree of this reduction (Bieniawski, 1989, 1973). To determine joint spacing values for each discontinuity system, we used the dedicated tool within DSE software (Riquelme *et alii*, 2015), which takes as input the relative position of each joint (considered to be non-persistent) and measures the orthogonal distances between them. This analysis was performed on the discontinuities derived from the photogrammetric point cloud obtained with the Matrice 200 sensor at a distance of 15 metres. Normal spacing values were also exploited to compute the Jv, later used for defining the RQD value, as well as the mean and maximum rock block volumes (Palmstrom, 2005).

The Rock Mass Rating (RMR) is a widely used geomechanical classification system for evaluating the quality and condition of rock masses in tunnels, mines, slopes, and foundations. Developed by (Bieniawski, 1989), the RMR system has been successfully applied in civil and rock engineering projects worldwide for over four decades. In this study, we employed the RMR89 version, which considers six parameters: *i*) rock material strength: unconfined compressive strength (UCS) or point load strength index (PLSI), *ii*) Rock Quality Designation (RQD), *iii*) discontinuity spacing, iv) discontinuity conditions (persistence, aperture, roughness, infilling, and weathering), *v*) groundwater conditions, and *vi*) discontinuity orientation. In our assessment, we derived the RQD and spacing values effectively through point cloud analysis, while other parameters were manually determined. For the RMR calculation, we used the QuickRMR computer application (Kundu *et alii*, 2020), which uses continuous functions to remove subjectivity from the rating scheme. It is important to note that RMR values may vary across different parts of the rock mass. Due to limited physical access to the entire area for investigations, there may be uncertainty in some parameter values. The adjustment rating for discontinuity orientation was not considered in this calculation, as it can vary along the slope.

- *Kinematic susceptibility*

Kinematic analysis is employed to evaluate the spatial distribution of potential failure mechanisms along rock slopes. The Markland test (Markland, 1972) is used to determine the kinematic instability of rock blocks through the examination of their bounding discontinuity systems. While kinematic analysis alone cannot fully explain all processes governing rock mass instability, it effectively identifies geometrically unstable blocks that are highly susceptible to failure, even with minimal triggering events. The analysis of photogrammetric and/or LiDAR point clouds provides precise topographic data and rock discontinuity parameters, enabling a detailed assessment of slope stability. In this study, we employed a 2D GIS-based computational application called GISMR (Kundu *et alii*, 2023) to identify zones susceptible to rock block detachment. The GISMR application utilises a pixel-based GIS approach to calculate the kinematic susceptibility of each pixel, taking into account discretized information on slope and discontinuity orientation. The integration of the derived friction angle with the geometric characteristics of discontinuities and slope face orientations allows for a comprehensive evaluation of potential failure modes.

Photomonitoring

Photomonitoring, leveraging optical and multispectral sensors, is essential for monitoring terrain changes and assessing rockfall hazards, especially along transportation corridors and steep, difficult-to-access rock faces. By using an aerial platform, this study capitalised on the flexibility in capturing high-resolution images from different angles, a capability particularly valuable in inaccessible locations like the vertical rock faces in Minori and Maiori. Compared to satellite imagery, UAV-based surveys provide superior spatial and temporal resolutions and allow the generation of photogrammetric 3D models that were rotated and orthorectified to produce front-facing orthomosaics of these rock faces (Figure 7). The orthomosaics were acquired in February 2023 and June 2023, thus providing the basis for Change Detection (CD) analysis to monitor slope evolution and detect potential detachment or structural changes (Cosentino *et alii*, 2023).

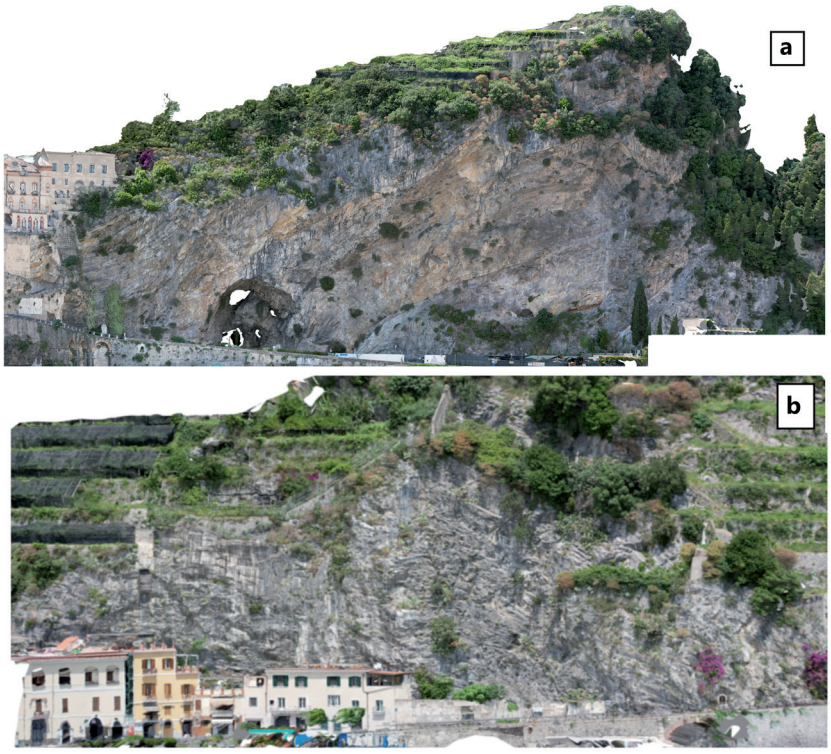

Fig. 7 - Orthomosaics depicting the slopes surveyed in localities Maiori (a) and Minori (b), and analysed by Photomonitoring techniques

The photomonitoring workflow included pre-processing for geometric corrections, co-registration of sequential images, CD analysis, and post-processing for result validation. This study used IRIS software version 23.0 (developed by NHAZCA S.r.l.), which employs the Structural Similarity Index Method (SSIM) to assess pixel-by-pixel changes by comparing brightness, contrast, and structural patterns (Sara *et alii*, 2019; Wang & Bovik, 2002). The SSIM equation, as shown below, evaluates image similarity on a scale of 0 to 1, with 1 indicating no change and 0 indicating the total change (Cosentino *et alii*, 2024).

$$SSIM(x,y) = [l(x,y)]^{\alpha} [c(x,y)]^{\beta} [s(x,y)]^{\gamma}$$

where $l(x,y)$ denotes luminance, comparing brightness; $c(x,y)$ represents contrast, comparing intensity ranges; and $s(x,y)$ reflects structural similarity. Constants α, β, and γ modulate the influence of each component. Using a 32-pixel moving window, the SSIM algorithm generated raster maps with values ranging from green (SSIM = 1, indicating no change) to blue (SSIM = 0, indicating total change), highlighting zones of significant structural alteration (Mastrantoni *et alii*, 2024).

The SSIM approach was chosen over other quality assessment techniques (*e.g.*, Mean Squared Error, UIQI, PSNR) due to its sensitivity to structural details. Through photomonitoring of orthoimages and DEMs derived from UAV data, changes in elevation and radiometric properties were analysed over time, forming a robust basis for supporting rockfall hazard assessment (Zocchi *et alii*, 2023).

RESULTS

3D point clouds comparison

This section presents the three-dimensional point clouds, and their derived features obtained from the surveys conducted in Minori and Maiori. Table 2 provides a comprehensive list of all the point clouds that were reconstructed and analysed for this project.

Site	Tool	Technique	Distance of acquisition (m)	Resolution (mm)
Maiori	Drone Mavic 3	Photogrammetry	30	8
Maiori	Drone Matrice 200	Photogrammetry	30	5
Maiori	TLS	LiDAR	100	30
Minori	Drone Mavic 3	Photogrammetry	15	8
Minori	Drone Mavic 3	Photogrammetry	35	11
Minori	Drone Matrice 200	Photogrammetry	15	5
Minori	Drone Matrice 200	Photogrammetry	35	9
Minori	TLS	LiDAR	50	15

Tab. 2 - List of 3D point clouds and their properties. The term resolution refers to the mean distance between two neighbouring points

To identify and quantify any differences between the photogrammetric and LiDAR products, two point clouds of the Minori slope acquired on the same day were compared. The quantitative analysis of the distances between the clouds is

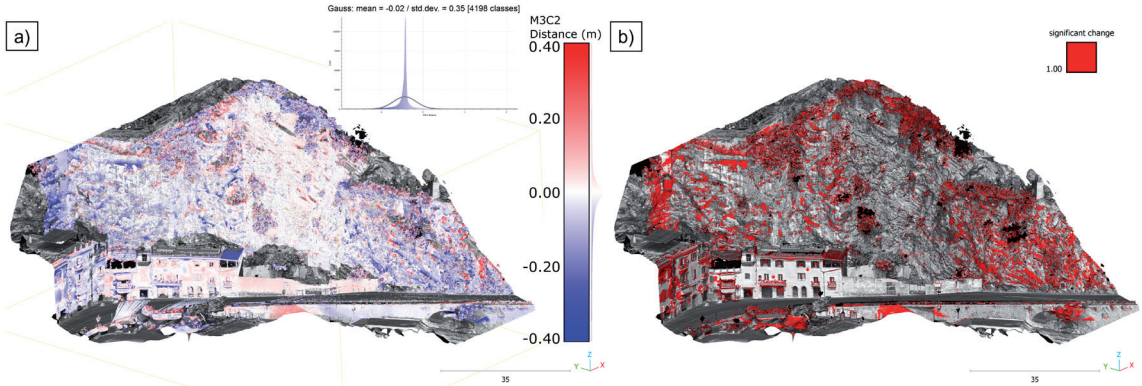

Fig. 8 - Point cloud distances in metres with relative histogram (a) and significant changes (i.e., > 0.2m) (b) between the photogrammetric and LiDAR point clouds both acquired on 7 June 2023 for the Minori rock face

presented in Figure 8a. Furthermore, all points showing significant distances are grouped and highlighted in Figure 8b. The comparison between the photogrammetric and LiDAR point clouds for the sub-vertical rock face in Minori reveals, albeit to a very limited range, differences distributed throughout the scanned area. Most of these differences can be attributed to vegetation. In contrast, others are due to bedding planes that are absent in the LiDAR cloud, as they were in the shadow of the acquisition point. Additionally, some differences are localised where metal nets are present along the rock surface.

The manual investigation of the discontinuity network for the Minori rock slope resulted in a total of 45 measures that were aggregated in three different joint sets. Figure 9a shows the discontinuity poles plotted on a Schmidt stereonet projection with the estimated density concentrations.

The physical measurements were further complemented by virtual measurements of the discontinuity orientations identified in the point cloud. The stereoplot of the 150 poles to planes obtained is presented in Figure 9b.

For the areas of interest A1 and A2, the semi-automatic discontinuity extraction resulted in four joint sets identified in both the UAV- and TLS-derived point cloud (Figure 10 and Figure 11). However, a certain discrepancy is observed between the results from A1, where the discontinuity poles from the TLS point cloud do not perfectly align with those derived from the photogrammetric point cloud acquired at a distance of 15 meters.

The results for the various sensor-distance combinations of drone-based photogrammetry are shown in Figure 12. Four discontinuity families were identified for all the explored combinations. However, some differences are present in the distribution of densities and the orientation of the principal poles automatically assigned by the software. Specifically, the stereoplots presented in Figure 13 show that the principal poles of the discontinuity families are consistent in both orientation and density. However, the geostructural analysis of the point cloud acquired with the DJI Mavic drone from a distance of 35 meters reveals a lower density of points corresponding to bedding surfaces with an orientation of 198/25. Consequently, unlike the other point clouds where the higher density principal pole is the bedding strata, in this case, it is assigned to the slope face, although no significant difference is observed in the orientations of the principal poles.

Rockfall stability

The normal spacing values obtained for each joint set within the study areas A1 and A2 are presented as column graphs (Figure 14). The automatic spacing measurements demonstrate an approximate log-normal distribution pattern with values ranging from 0.06 m

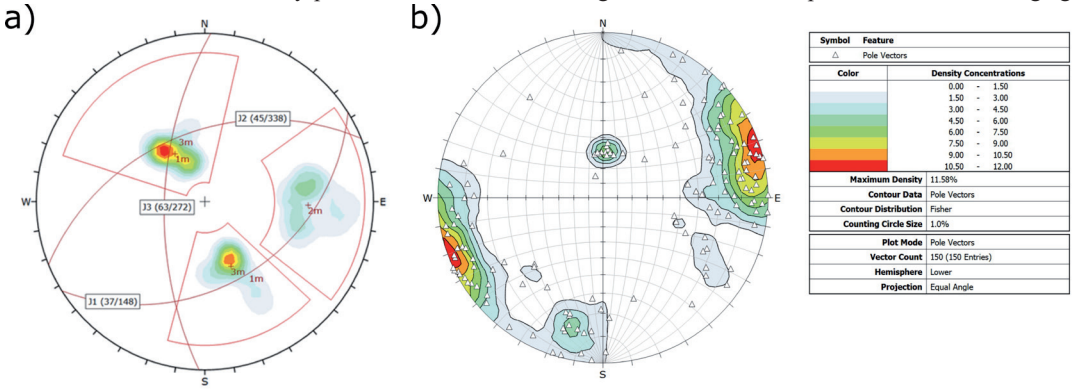

Fig. 9 - Stereoplot of field measured discontinuity poles (a), and virtually measured poles (b)

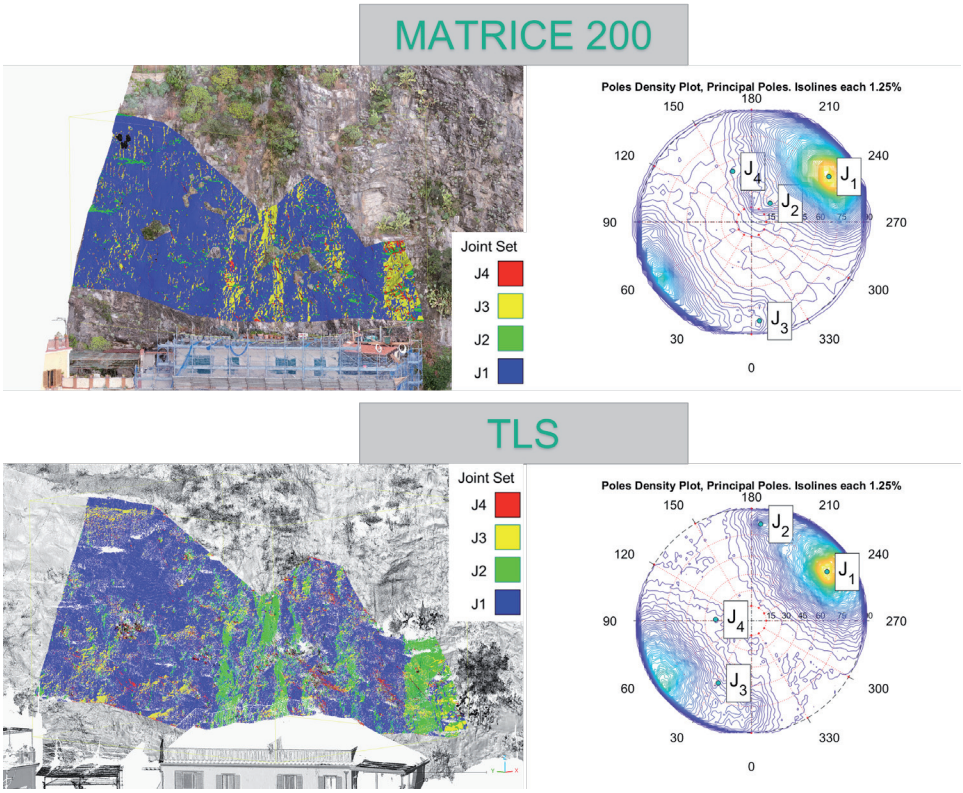

Fig. 10 - Discontinuities extracted from the Matrice 200 (top) and TLS-derived (bottom) point clouds in area A1

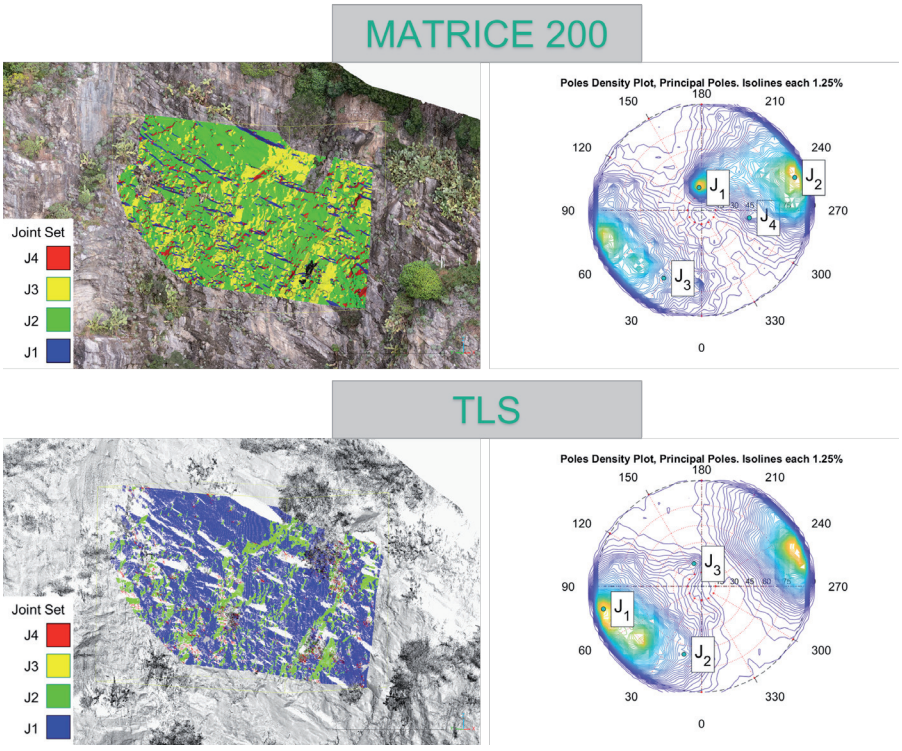

Fig. 11 - Discontinuities extracted from the Matrice 200 and TLS-derived point clouds in area A2

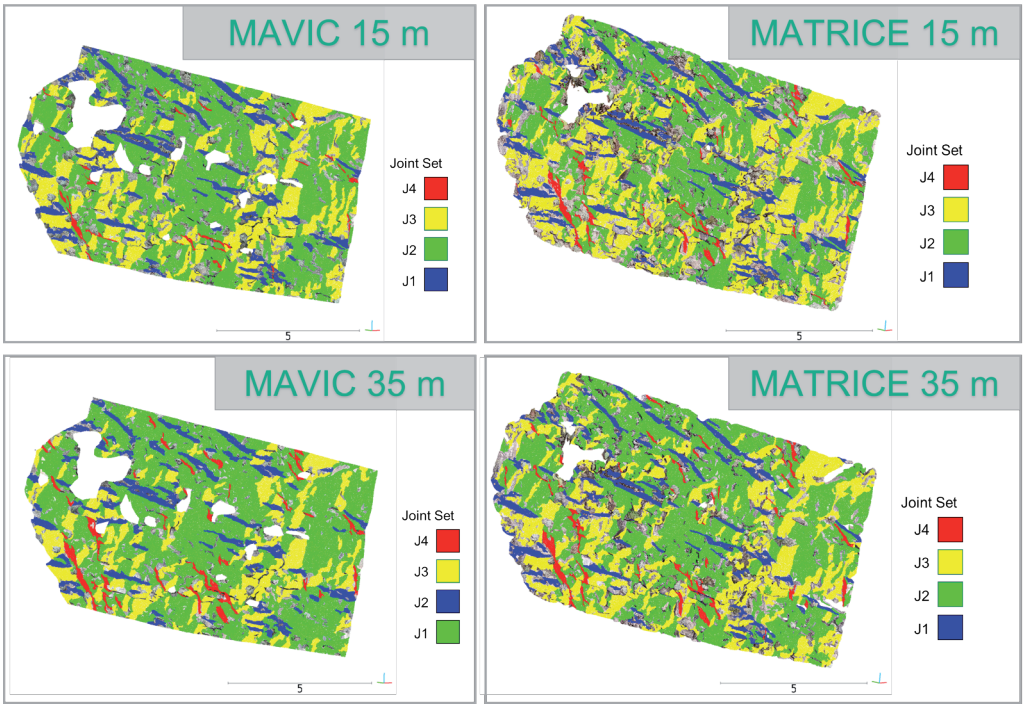

Fig. 12 - Geostructural classification of the A2 zone using the Matrice 200 and Mavic point clouds obtained at 15m and 35m of acquisition distance

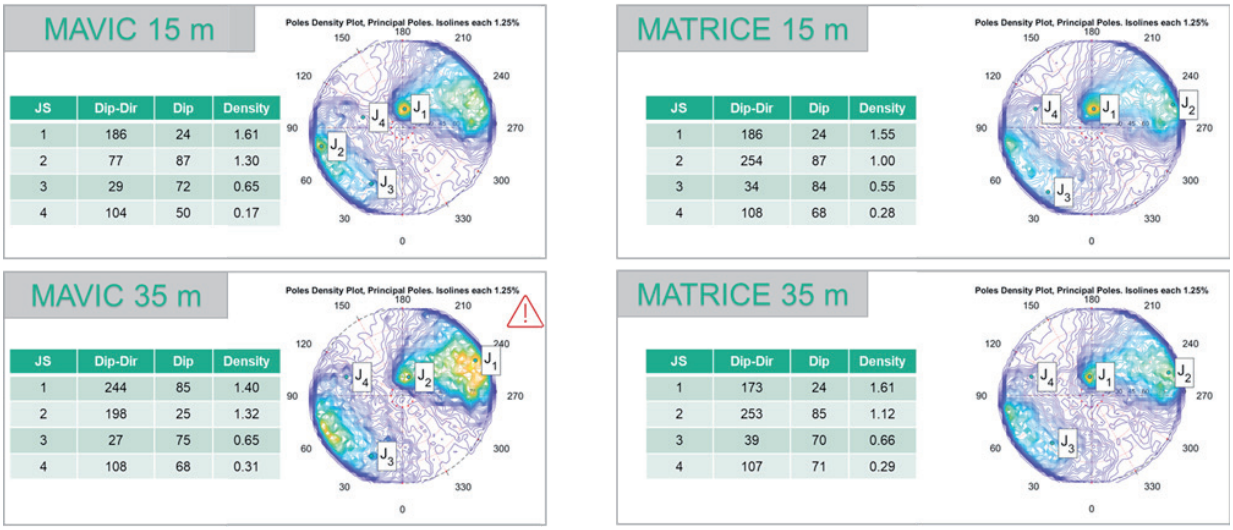

Fig. 13 - . Stereoplots and summary tables of discontinuity orientations for the different sensor-distance combinations

to 1.03 m. Based on the obtained spacing values, the volumetric joint count (Jv), Rock Quality Designation (RQD), and block volume were calculated. The analysis yielded a Jv value of 14, an RQD value of 68, and a mean volume of rock blocks of 4.69×10^{-2} m (Table 3). The basic Rock Mass Rating (RMR) was calculated using the QuickRMR computer application (Kundu *et alii*, 2020), incorporating parameters obtained through both physical measurements and point cloud analysis. The analysis yielded a basic RMR value of 57, corresponding to Class III rock mass quality.

	Spacing [m]				Jv	RQD [%]	Bock volume [m3]	Class
	J1	J2	J3	J4				
Mean	0.38	0.34	0.20	0.28	14	68	4.69×10^{-2}	Moderate
Max	1.03	0.86	0.62	0.76	5	98	9.835×10^{-1}	Big

Tab. 3 - Summary of rock mass parameters derived from point cloud analysis, including estimated mean and maximum values of normal spacing, joint volume count, rock quality designation, block volume, and block class

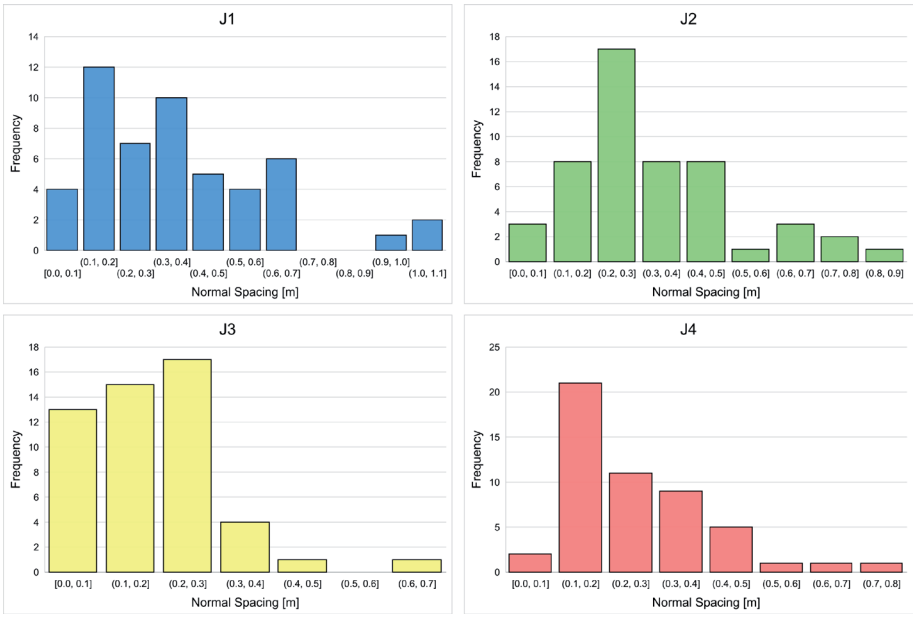

Fig. 14 - Normal spacing values distribution in A1 and A2

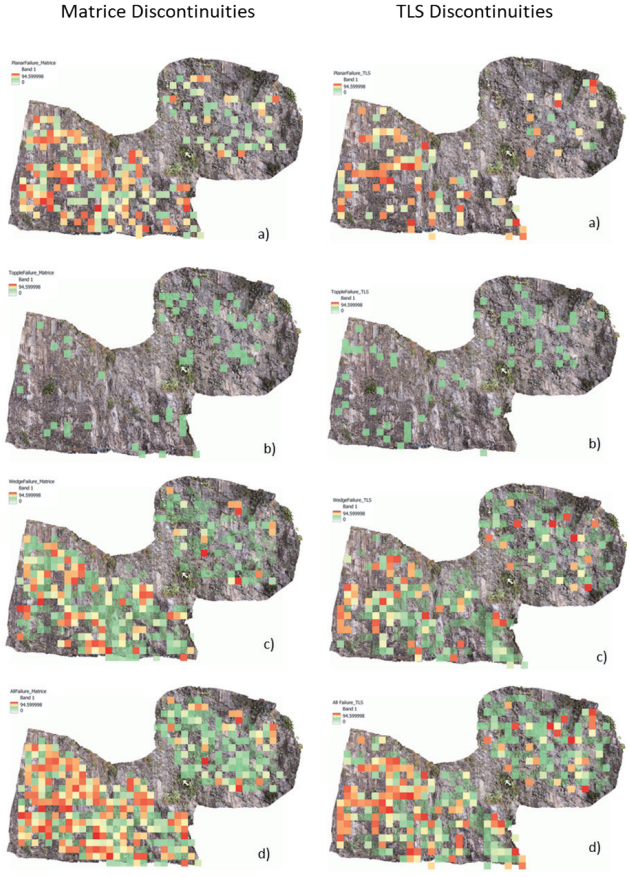

Fig. 15 - Kinematic susceptibility maps for photogrammetric and TLS-based point clouds

The slope friction angle, determined through tilt angle tests performed on multiple non-cohesive joint interfaces at different locations, ranged from 27° to 32°, which is consistent with B*ieniawski*'s (1993) correlation. The kinematic analysis results were generated in raster format, where each pixel contains information about the maximum hazard value. The lateral limits for planar and toppling failures in the kinematic analysis were set according to generally accepted values: 20° for planar sliding and 10° for toppling failures. The kinematic analysis results were overlaid on an RGB level for better visualisation. The results for a 1 m pixel resolution are presented in Figure 15. The kinematic susceptibility derived from the Matrice 200 UAV sensor point clouds is shown side-by-side with the results obtained from the TLS-derived point clouds for planar, wedge, flexural toppling, and all three failure modes combined. The legend represents the susceptibility value ranging from 0 to 100 in a heatmap. Green corresponds to a low hazard value, while red indicates a high hazard.

Orthophoto change detection

The change detection (CD) analyses allowed us to identify areas affected by changes over the investigated period across all four orthomosaics of the rock masses in Minori and Maiori. To ensure that the analyses reflected only the significant changes in the rock slopes, we cropped each orthomosaics to exclude peripheral elements that could introduce noise, such as scaffolding removal or changes in road traffic. Figure 16 shows the CD results for the Minori rock face, where high SSIM values (green) predominantly indicate stability, with no significant detachment processes observed. Areas with lower SSIM values are mostly attributed to vegetation changes or shadow effects on the rock surface.

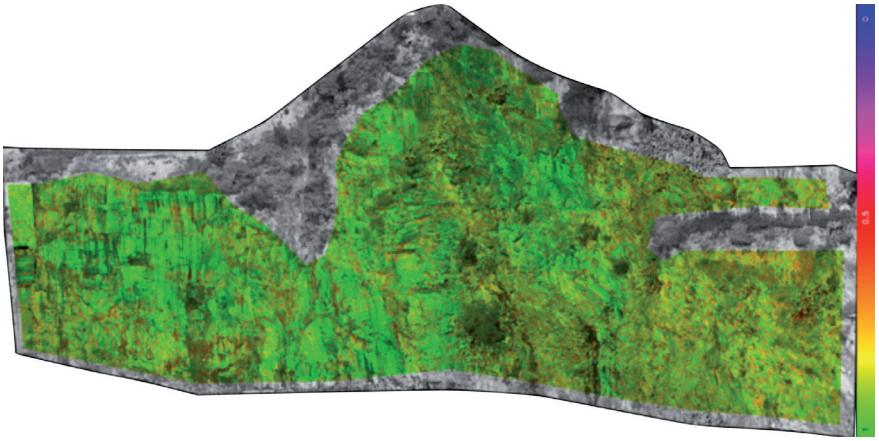

Fig. 16 - Change detection (CD) results for the rock face in Minori. High SSIM values (green) indicate no significant detachment processes, suggesting overall stability. Areas with lower SSIM values are primarily associated with vegetation changes or shadow effects on the rock surface

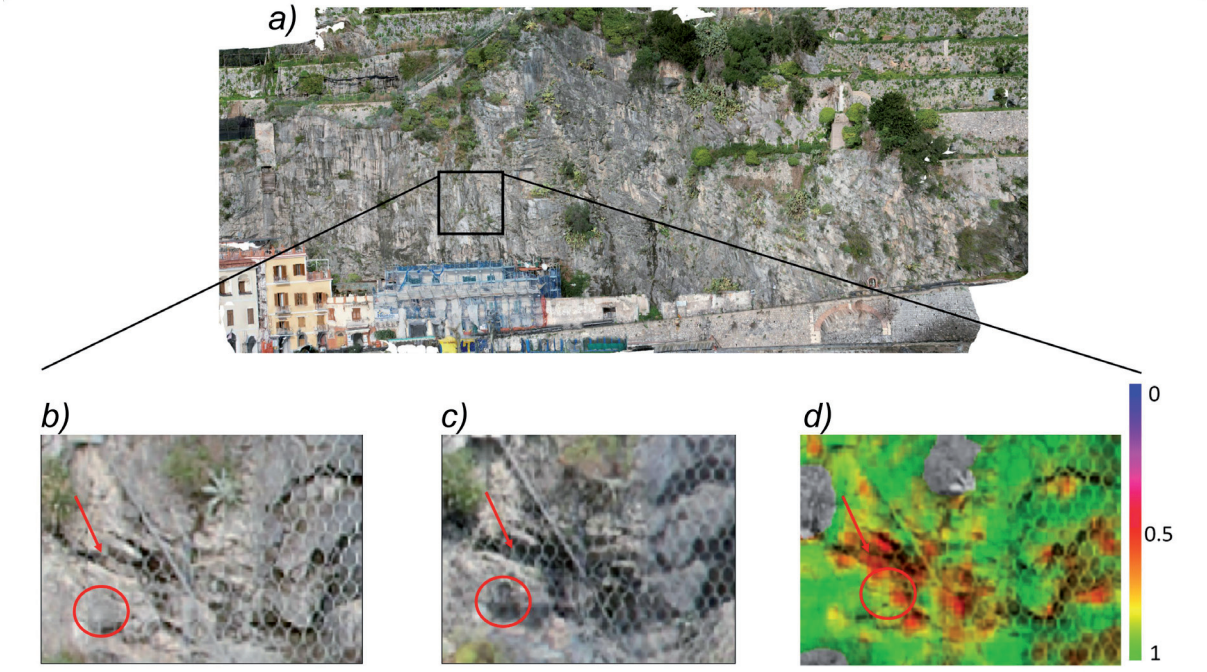

Fig. 17 - Detailed view of the orthophoto collected for the Minori rock face: orthophoto related to the February 2023 photogrammetric survey (a, b); June 2023 orthophoto (c); example result of the Change Detection analysis (d). In the zoomed-in areas, small detachment events are visible, highlighted by the red circles and arrows, corresponding to the lowest SSIM values (red tones). Areas with moderately lower SSIM values (yellow) may indicate minor changes due to shadows or vegetation variation

A detailed view in Figure 17 highlights a minor rockfall event near the edge of the Minori rock face adjacent to the inhabited area. Low SSIM values (in red) mark the detachment of several blocks in a section with rockfall nets installed. Generally, only a few limited detachment phenomena were observed following the interpretation of the results, suggesting the overall stability of the rock faces. Some sporadic false positives, related to shadow effects and vegetation changes, were noted. However, this apparent stability could be due to the short time span between the two UAV acquisitions (three months), which may limit the detection of significant detachment events.

DISCUSSION

Integrating aerial photogrammetry and terrestrial laser scanning enabled the reconstruction of 3D digital models of the rock slopes near the urban centres of Minori and Maiori. These 3D point clouds represent the surveyed object at a 1:1 scale, facilitating various geometric analyses, including

quantitative comparison between the point clouds.

Comparative analysis revealed that photogrammetric products of complex scenarios, such as sub-vertical rock slopes, may be subject to localised deformations. This limitation is primarily attributed to the physical impossibility of installing reference points along the outcrop, restricting GNSS measurements to the road level. In such contexts, validation of photogrammetric point clouds necessitates quantitative comparison with LiDAR data, which remains free from artefacts even in the absence of known reference points. Significant differences were observed in the representation of vegetation and protective mesh structures between the two techniques. Structure from Motion algorithms struggled to accurately capture the geometric complexity of these features, resulting in overly smoothed and approximated forms. In contrast, LiDAR data enabled more effective discrimination of distances, leading to quantifiable geometric differences of up to 40 cm in mesh-covered areas. Furthermore, the TLS sensor's ability to record laser pulse amplitude data facilitated rapid and effective filtering of vegetation and metallic meshes, a process that is considerably more time-consuming and computationally intensive for photogrammetric point clouds.

Conversely, given the LiDAR scan positions, point clouds present inherent limitations related to line-of-sight occlusions, resulting in shadow zones and data gaps, particularly in areas with overhanging strata and south-dipping surfaces. To minimize this phenomenon, multi-station surveys capable of providing 360-degree coverage of the target object are typically necessary. However, this comprehensive coverage is not always achievable, particularly in natural settings. This limitation is effectively overcome by aerial photogrammetry, which enables image acquisition from any point in three-dimensional space.

Another fundamental capability of point cloud analysis is the extraction of normal vectors, enabling the identification of discontinuities within the rock mass (Riquelme *et alii*, 2015, 2014). While traditional manual measurements are essential, they are often constrained by accessibility, time requirements, and subjectivity. Point clouds offer an efficient alternative, allowing the extraction of orientation data, effectively enabling the measurement of hundreds of discontinuity surfaces directly from the digital outcrop model, with manual compass measures serving as validation (Francioni *et alii*, 2019). Along the Minori rock slope, four discontinuity families were identified and classified as bedding planes, slope face, and minor fractures. The analysis included a comparison of 150 manually extracted discontinuity orientations from the photogrammetric point cloud with both field measurements and semi-automatic results, revealing excellent correlation, particularly for bedding planes, slope faces, and J3 discontinuities. Comparative analysis of discontinuities derived from photogrammetric and TLS point clouds revealed significant differences, primarily due to the latter's limited representation of bedding surfaces. This limitation has substantial implications for rock mass characterization, as underestimating bedding plane frequency can lead to overestimated spacing values and, consequently, block sizes (Robiati *et alii*, 2023). The kinematic analysis results obtained in this study further stressed this discrepancy. Analyses using TLS-derived joint data tend to indicate lower or absent susceptibility values in areas where SfM-derived data analysis shows higher susceptibility. This observation highlights a critical limitation in relying solely on TLS data for comprehensive slope stability assessment, particularly in complex geometric settings where it is impossible to perform the appropriate scanning positions to achieve a thorough representation of the rock mass (Pagano *et alii*, 2020).

To further investigate the impact of point cloud resolution on discontinuity extraction, photogrammetric surveys were conducted using different UAV platforms and flight distances. Results demonstrated that the ratio between sensor resolution and acquisition distance is proportional to point cloud density, significantly influencing the semi-automatic extraction of discontinuity sets (Daghigh *et alii*, 2022). Generally, higher sensor resolution combined with shorter acquisition distances yields greater point cloud density. However, it is crucial to consider that at a constant field of view (FOV), decreasing the distance to the target necessitates a larger number of photographs to reconstruct the digital model. Therefore, an optimal balance must be established between flight time and required point cloud density to ensure efficient data collection while maintaining adequate resolution for structural analysis.

The comprehensive spatial coverage provided by the virtual outcrop models enhances the estimation of crucial joint properties, including mean spacing, persistence, admissible rock volumes, and overall accuracy of rock mass quality. This capability represents a significant advancement over traditional field methods, particularly in areas with limited accessibility, and provides a more robust foundation for subsequent geomechanical analyses and hazard assessments (Žabota *et alii*, 2023). It enabled precise estimation of Rock Quality Designation (RQD), volumetric joint count (Jv), and in-situ block volumes. However, it is crucial to recognize the distinction between remotely measurable and non-remotely

Can be acquired effectively with acceptable error	Acquired with difficulty and imprecision	Can not be acquired
Normal spacing	Persistence/length	Resistance of intact rock
RQD	Roughness	Separation
	Seepage conditions (LiDAR reflectivity)	Infilling
		Alteration/weathering

Tab. 4 - Degree of feasibility of RMR parameters to be derived from photogrammetric and/or TLS point clouds

measurable geomechanical parameters, as certain properties still require direct field measurements or observations (Table 4). The obtained RMR value represents an average characterization of the rock mass quality; in fact, this value may exhibit spatial variability across different sections of the rock mass. Due to limited physical accessibility to certain portions of the study area, there is inherent uncertainty in some parameter values. The adjustment rating was not incorporated in this calculation due to its potential variation along the slope. This understanding is essential for developing integrated approaches that combine remote sensing capabilities with traditional field investigations to achieve comprehensive rock mass characterization.

This study highlights the potential of change detection (CD) methodologies for orthomosaics generated through photogrammetric techniques using UAV platforms. Our analyses revealed that the resolution of these orthophoto plays a crucial role in determining the accuracy and reliability of CD results. Higher resolution requires greater computational resources while enabling more precise detection of changes in rock face conditions.

The results of this work show that high-resolution orthophotos allow for effective discrimination of vegetation and facilitate its filtering where it may otherwise represent a limitation. This capability is critical for improving the precision of the analysis, especially in vegetated areas. Additionally, high-resolution imagery proved instrumental in assessing the effectiveness of protective systems, such as rockfall nets. In this specific application, a small tear in the net was detected, demonstrating the level of detail achievable. Notably, the presence of the net itself did not impede the analysis.

In the field of image quality assessment for CD analysis, the Structural Similarity Index Measure (SSIM) has emerged as a preferred technique due to its ability to evaluate perceived image quality by comparing structural similarities between original and derived images. Other metrics, such as Mean Squared Error (MSE), Universal Image Quality Index (UIQI), Peak Signal-to-Noise Ratio (PSNR), Human Vision System (HVS), and Feature Similarity Index Method (FSIM), have also proven useful in measuring image similarity (Sara *et alii*, 2019). Among these, SSIM stands out for its reliability and accuracy, making it particularly effective for monitoring applications, as supported by Kim *et alii*, 2019. The results of this study further validate SSIM's potential, as it consistently delivered high-quality outcomes in detecting changes on rock slopes.

The reliance on optical sensors for UAV-based photogrammetry, however, introduces limitations under adverse weather conditions. Cosentino *et alii*, (2023) demonstrated that combining thermal (TIR) and optical sensors on UAV platforms can enhance monitoring effectiveness, providing complementary data that mitigate these limitations. Additionally, Massi *et alii*, (2023) highlighted the potential of visible-light/near-infrared (VIS/NIR) sensors to further expand monitoring capabilities. Although these techniques currently operate within a 2D framework and cannot quantify rockfall volumes, they offer innovative, low-cost, and low-impact solutions for hazard assessment based on multi-temporal inventories rather than kinematic tests (Mastrantoni *et alii*, 2024).

By leveraging UAV platforms, this study underscores the importance of integrating multiple sensing technologies for comprehensive rock slope monitoring. UAV photogrammetry provides a cost-effective solution for generating high-resolution orthomosaics, while thermal and VIS/NIR imaging deliver valuable complementary data, particularly under challenging environmental conditions. Future research should focus on optimizing these combined methodologies to enhance the consistency and accuracy of rock slope monitoring and hazard evaluation.

CONCLUSION

This study demonstrates the significant potential and limitations of remote sensing technologies for geomechanical characterization of rock masses and photomonitoring of hazardous areas affecting transportation infrastructure, particularly in sub-vertical rock slopes where traditional monitoring methods may be limited or impractical.

Point clouds of steep natural slopes obtained through aerial photogrammetry may exhibit topographic discrepancies when compared to LiDAR point clouds acquired via Terrestrial Laser Scanning. However, UAV-based systems ensure comprehensive coverage of the area of interest, overcoming the limitations of ground-based approaches. Semi-automatic geostructural analyses performed on photogrammetric point clouds, acquired though different sensors and capture distances, showed no significant critical differences in results, apart from minor variations in joint density. Nevertheless, the presence of rockfall protection nets adjacent to the rock mass represents a significant source of error in the photogrammetric reconstruction process, resulting in a single smoothed and approximated surface that includes both the rock mass and overlying nets. This limitation is less problematic in laser scanner surveys. On the other hand, terrestrial laser scanning surveys present limitations in steep mountainous contexts where different scan positions relative to the investigated scenario are not available. In certain contexts, the integration of LiDAR and aerial photogrammetry provides robust geostructural analyses through the mutual compensation of their strengths. While semi-automatic geostructural surveys on 3D point clouds are preferable to manual field surveys, they must always be guided and validated by site data.

Photomonitoring emerges as an innovative technique for obtaining information on changes (Change Detection) and displacements (Digital Image Correlation) of natural slopes, enabling both qualitative and quantitative hazard assessment.

These findings underscore the importance of integrating multiple remote sensing technologies for comprehensive slope

stability assessment and monitoring, particularly where traditional surveying methods may be limited or impractical. The integration of multiple data sources can help overcome the inherent limitations of individual methods, providing a more comprehensive understanding of static and dynamic factors. The selection of appropriate survey techniques should therefore consider not only the general precision of the method but also its effectiveness in capturing the full range of slope parameters and any possible slope failure. Understanding the limitations and complementary strengths of the different remote sensing technologies enables more informed decision-making in slope stability assessment and monitoring programs, ultimately contributing to effective risk mitigation strategies for transportation networks.

Declaration of competing interest

The authors declare that they have no known competing financial interests or personal interest relationships that could have appeared to influence the work reported in this paper.

Authors Contribution

Giandomenico Mastrantoni: Conceptualization, Methodology, Software, Validation, Formal Analysis, Investigation, Data Curation, Writing-Original Draft Preparation, Writing-Review and Editing, Visualization.
Antonio Cosentino: Methodology, Software, Validation, Data Curation, Writing-Original Draft Preparation.
Marta Zocchi: Conceptualization, Methodology, Software, Validation, Investigation, Writing-Original Draft Preparation, Visualization.
Jagadish Kundu: Software, Validation, Investigation, Data Curation, Writing-Review and Editing. *Angelo Dandini:* Writing-Review and Editing.
Maurizio Martino: Writing-Review and Editing.
Alfredo Montagna: Writing-Review and Editing, Validation.
Gabriele Scarascia Mugnozza: Validation, Writing-Review and Editing, Project Administration, Funding Acquisition.
Paolo Mazzanti: Validation, Writing-Review and Editing, Supervision, Project Administration, Funding Acquisition.

REFERENCES

Abellán A., Oppikofer T., Jaboyedoff M., Rosser N.J., Lim M. & Lato M.J. (2014) - *Terrestrial laser scanning of rock slope instabilities*. Earth Surface Processes and Landforms, **39**: 80-97. https://doi.org/10.1002/esp.3493

Barton N. (2013) - *Shear strength criteria for rock, rock joints, rockfill and rock masses: Problems and some solutions*. Journal of Rock Mechanics and Geotechnical Engineering, **5**: 249-261. https://doi.org/10.1016/j.jrmge.2013.05.008

Barton N. & Choubey V. (1977) - *The shear strength of rock joints in theory and practice*. Rock Mechanics, **10**: 1-54. https://doi.org/10.1007/BF01261801

Bieniawski Z.T. (1989) - *Engineering rock mass classifications: a complete manual for engineers and geologists.* Mining, Civil, and Petroleum Engineering. John Wiley & Sons.

Bieniawski Z.T. (1973) - *Engineering classification of jointed rock masses.* Civil Engineering= Siviele Ingenieurswese 1973: 335-343.

Carannante G., Ruberti D. & Sirna M. (2000) - *Upper Cretaceous ramp limestones from the Sorrento Peninsula (southern Apennines, Italy): micro- and macrofossil associations and their significance in the depositional sequences*. Sedimentary Geology, **132**: 89-123. https://doi.org/10.1016/S0037-0738(00)00004-X

Carrivick J.L., Smith M.W. & Quincey D.J. (2016) - *Structure from Motion in the Geosciences.* John Wiley & Sons.

Coggan J.S., Wetherelt A., Gwynn X.P. & Flynn Z.N. (2007) - *Comparison of Hand-mapping With Remote Data Capture Systems For Effective Rock Mass Characterisation*. Presented at the 11th ISRM Congress, OnePetro.

Cosentino A., Brunetti A. & Mazzanti P. (2024) - *Photomonitoring as a tool for monitoring landslides: a technology within everyone's reach*. Transportation Research Record 03611981241270173. https://doi.org/10.1177/03611981241270173

Cosentino A., Marmoni G.M., Fiorucci M., Mazzanti P., Scarascia Mugnozza G. & Esposito C. (2023) - *Optical and thermal image processing for monitoring rainfall triggered shallow landslides: insights from analogue laboratory experiments.* Remote Sensing, **15**: 5577. https://doi.org/10.3390/rs15235577

Daghigh H., Tannant D.D., Daghigh V., Lichti D.D. & Lindenbergh R. (2022) - *A critical review of discontinuity plane extraction from 3D point cloud data of rock mass surfaces.* Computers & Geosciences, **169**: 105241. https://doi.org/10.1016/j.cageo.2022.105241

Farmakis I., Marinos V., Papathanassiou G. & Karantanellis E. (2020) - *Automated 3D Jointed Rock Mass Structural Analysis and Characterization Using LiDAR Terrestrial Laser Scanner for Rockfall Susceptibility Assessment: Perissa Area Case (Santorini).* Geotech. Geol. Eng., **38**: 3007-3024. https://doi.org/10.1007/s10706-020-01203-x

Ferrero A.M., Forlani G., Roncella R. & Voyat H.I. (2009) - *Advanced Geostructural Survey Methods Applied to Rock Mass Characterization.* Rock Mech. Rock. Eng., **42**: 631-665. https://doi.org/10.1007/s00603-008-0010-4

Francioni M., Antonaci F., Sciarra N., Robiati C., Coggan J., Stead D. & Calamita F. (2020) - *Application of Unmanned Aerial Vehicle Data and Discrete Fracture Network Models for Improved Rockfall Simulations.* Remote Sensing, **12**: 2053. https://doi.org/10.3390/rs12122053

Francioni M., Stead D., Sciarra N. & Calamita F. (2019) - *A new approach for defining Slope Mass Rating in heterogeneous sedimentary rocks using a combined remote sensing GIS approach*. Bull. Eng. Geol. Environ., **78**: 4253-4274. https://doi.org/10.1007/s10064-018-1396-1

Gallo I.G., Martínez-Corbella M., Sarro R., Iovine G., López-Vinielles J., Hérnandez M., Robustelli G., Mateos R.M. & García-Davalillo

J.C. (2021) - *An Integration of UAV-Based Photogrammetry and 3D Modelling for Rockfall Hazard Assessment: The Cárcavos Case in 2018 (Spain)*. Remote Sensing, **13**: 3450. https://doi.org/10.3390/rs13173450

Gigli G. & Casagli N. (2011) - *Semi-automatic extraction of rock mass structural data from high resolution LIDAR point clouds*. International Journal of Rock Mechanics and Mining Sciences, **48**: 187-198.

Girardeau-Montaut D. (2006) - *Détection de changement sur des données géométriques tridimensionnelles (phdthesis).* Télécom ParisTech.

Goodman R.E. (1991) - *Introduction to Rock Mechanics*. John Wiley & Sons.

Guerriero L., Di Martire D., Calcaterra D. & Francioni M. (2020) - *Digital image correlation of Google Earth images for Earth's surface displacement estimation*. Remote Sensing, **12**: 3518. https://doi.org/10.3390/rs12213518

Guzzetti F., Reichenbach P. & Ghigi S. (2004) - *Rockfall hazard and risk assessment along a transportation corridor in the Nera Valley, Central Italy.* Environmental Management, **34**: 191-208. https://doi.org/10.1007/s00267-003-0021-6

Iannace A., Capuano M. & Galluccio L. (2011) - *"Dolomites and dolomites" in Mesozoic platform carbonates of the Southern Apennines: Geometric distribution, petrography and geochemistry.* Palaeogeography, Palaeoclimatology, Palaeoecology, **310**: 324-339. https://doi.org/10.1016/j.palaeo.2011.07.025

Iannace A., Merola D., Perrone V., Amato A., Cinque A., Santacroce R. & D'Argenio B. (2015) - *Note Illustrative Della Carta Geologica d'Italia Alla Scala 1: 50.000 Fogli 466-485 Sorrento-Termini.* Servizio Geologico d'Italia, ISPRA, 204.

Jaboyedoff M., Abellán A., Carrea D., Derron M.-H., Matasci B. & Michoud C. (2018) - *Mapping and Monitoring of Landslides Using LIDAR, in: Natural Hazards. CRC Press.*

James M.R. & Robson S. (2012) - *Straightforward reconstruction of 3D surfaces and topography with a camera: Accuracy and geoscience application.* Journal of Geophysical Research: Earth Surface 117. https://doi.org/10.1029/2011JF002289

Kim B.H., Cai M., Kaiser P.K. & Yang H.S. (2007) - *Estimation of block sizes for rock masses with non-persistent joints.* Rock Mech. Rock Eng., **40**: 169-192. https://doi.org/10.1007/s00603-006-0093-8

Kim D., Balasubramaniam A.S., Gratchev I., Kim S.R. & Chang S.H. (2019*)* - *Application of image quality assessment for rockfall investigation. vectors (x and y) 2, 1.* Proceedings of the 16th Asian Regional Conference on Soil Mechanics and Geotechnical Engineering: Geotechnique for Sustainable Development and Emerging Market Regions, ARC 2019. http://seags.ait.asia/16arc-proceedings/16arc-proceedings/

Kundu J., Mastrantoni G., Santicchia G., Cosentino A., Scarascia-Mugnozza G. & Mazzanti P. (2024) - *Advancing rock slope hazard assessment by remote sensing: the contribution of the Poggio Baldi landslide natural laboratory.* New Challenges in Rock Mechanics and Rock Engineering. CRC Press.

Kundu J., Sarkar K., Ghaderpour E., Scarascia Mugnozza G. & Mazzanti P. (2023*)* - *A GIS-based kinematic analysis for jointed rock slope stability: an application to Himalayan Slopes.* Land, **12**(2): 402. https://doi.org/10.3390/land12020402

Kundu J., Sarkar K., Singh A.K. & Singh T.N. (2020) - *Continuous functions and a computer application for Rock Mass Rating.* International Journal of Rock Mechanics and Mining Sciences, **129**: 104280. https://doi.org/10.1016/j.ijrmms.2020.104280

Luhmann T., Robson S., Kyle S. & Boehm J. (2019) - *Close-Range Photogrammetry and 3D Imaging, Close-Range Photogrammetry and 3D Imaging.* De Gruyter. https://doi.org/10.1515/9783110607253

Markland J.T. (1972) - *A useful technique for estimating the stability of rock slopes when the rigid wedge slide type of failure is expected (No. 19).* Inter-departmental Rock Mechanics Project, Imperial College of Science and Technology.

Massi A., Ortolani M., Vitulano D., Bruni V. & Mazzanti P. (2023) - *Enhancing the thermal images of the upper scarp of the Poggio Baldi Landslide (Italy) by physical modeling and image analysis.* Remote Sensing, **15**: 907. https://doi.org/10.3390/rs15040907

Mastrantoni G., Santicchia G., Cosentino A., Molinari A., Marmoni G.M. & Mazzanti P. (2024) - *Automatic photomonitoring analysis for spatio-temporal evaluation of rockfall failure hazard.* Engineering Geology, **339**: 107662. https://doi.org/10.1016/j.enggeo.2024.107662

Mazza D., Cosentino A., Romeo S., Mazzanti P., Guadagno F.M. & Revellino P. (2023) - *Remote Sensing Monitoring of the Pietrafitta Earth Flows in Southern Italy: An Integrated Approach Based on Multi-Sensor Data.* Remote Sensing, **15**: 1138. https://doi.org/10.3390/rs15041138

Mazzanti P., Bozzano F., Brunetti A., Caporossi P., Esposito C. & Mugnozza G.S. (2017*)* - *Experimental Landslide Monitoring Site of Poggio Baldi Landslide (Santa Sofia, N-Apennine, Italy), in: Mikoš, M., Arbanas, Ž., Yin, Y., Sassa, K. (Eds.), Advancing Culture of Living with Landslides.* Springer International Publishing, Cham: 259-266. https://doi.org/10.1007/978-3-319-53487-9_29

Mazzanti P., Brunetti A. & Bretschneider A. (2015) - *A New Approach Based on Terrestrial Remote-sensing Techniques for Rock Fall Hazard Assessment, in: Scaioni, M. (Ed.), Modern Technologies for Landslide Monitoring and Prediction,* Springer Natural Hazards. Springer, Berlin, Heidelberg: 69-87. https://doi.org/10.1007/978-3-662-45931-7_4

Mazzanti P., Caporossi P. & Muzi R. (2020*)* - *Sliding Time Master Digital Image Correlation Analyses of CubeSat Images for landslide Monitoring: The Rattlesnake Hills Landslide (USA).* Remote Sensing, **12**: 592. https://doi.org/10.3390/rs12040592

Pagano M., Palma B., Ruocco A. & Parise M. (2020*)* - *Discontinuity Characterization of Rock Masses through Terrestrial Laser Scanner and Unmanned Aerial Vehicle Techniques Aimed at Slope Stability Assessment.* Applied Sciences, **10**: 2960. https://doi.org/10.3390/app10082960

Palmstrom A. (2005) - *Measurements of and correlations between block size and rock quality designation (RQD).* Tunnelling and Underground Space

Technology, **20**: 362-377. https://doi.org/10.1016/j.tust.2005.01.005

Patacca E. & Scandone P. (2007) - *Geology of the southern Apennines.* Bollettino della Società Geologica Italiana, **7**: 75-119.

Peralta T., Menoscal M., Bravo G., Rosado V., Vaca V., Capa D., Mulas M. & Jordá-Bordehore L. (2024) - *Rock slope stability analysis using terrestrial photogrammetry and virtual reality on ignimbritic deposits.* Journal of Imaging, **10**: 106. https://doi.org/10.3390/jimaging10050106

Riquelme A., Cano M., Tomás R. & Abellán A. (2017) - *Identification of Rock Slope Discontinuity Sets from Laser Scanner and Photogrammetric Point Clouds: A Comparative Analysis.* Procedia Engineering, ISRM European Rock Mechanics Symposium EUROCK 2017, **191**: 838-845. https://doi.org/10.1016/j.proeng.2017.05.251

Riquelme A.J., Abellán A. & Tomás R. (2015) - *Discontinuity spacing analysis in rock masses using 3D point clouds*. Engineering Geology, **195**: 185-195. https://doi.org/10.1016/j.enggeo.2015.06.009

Riquelme A.J., Abellán A., Tomás R. & Jaboyedoff M. (2014) - *A new approach for semi-automatic rock mass joints recognition from 3D point clouds.* Computers & Geosciences, **68**: 38-52. https://doi.org/10.1016/j.cageo.2014.03.014

Robiati C., Eyre M., Vanneschi C., Francioni M., Venn A. & Coggan J. (2019) - *Application of Remote Sensing Data for Evaluation of Rockfall Potential within a Quarry Slope.* ISPRS International Journal of Geo-Information, **8**: 367. https://doi.org/10.3390/ijgi8090367

Robiati C., Mastrantoni G., Francioni M., Eyre M., Coggan J. & Mazzanti P. (2023) - *Contribution of High-Resolution Virtual Outcrop Models for the Definition of Rockfall Activity and Associated Hazard Modelling.* Land, **12**: 191. https://doi.org/10.3390/land12010191

Sapirstein P. (2016) - *Accurate measurement with photogrammetry at large sites*. Journal of Archaeological Science, **66**: 137-145. https://doi.org/10.1016/j.jas.2016.01.002

Sara U., Akter M. & Uddin M.S. (2019) - *Image Quality Assessment through FSIM, SSIM, MSE and PSNR—A Comparative Study*. Journal of Computer and Communications, **7**: 8-18. https://doi.org/10.4236/jcc.2019.73002

Seitz S.M., Curless B., Diebel J., Scharstein D. & Szeliski R. (2006) - *A comparison and evaluation of multi-view stereo reconstruction algorithms*. 2006 IEEE Computer Society Conference on Computer Vision and Pattern Recognition (CVPR'06). Presented at the 2006 IEEE Computer Society Conference on Computer Vision and Pattern Recognition (CVPR'06): 519-528. https://doi.org/10.1109/CVPR.2006.19

Spetsakis M.E. & *Aloimonos J. (Yiannis)* (1990) - *Structure from motion using line correspondences*. Int. J. Comput. Vision, **4**: 171-183. https://doi.org/10.1007/BF00054994

Tavani S., Iannace A., Mazzoli S., Vitale S. & Parente M. (2013) - *Late Cretaceous extensional tectonics in Adria: Insights from soft-sediment deformation in the Sorrento Peninsula (southern Apennines)*. Journal of Geodynamics, 68: 49-59. https://doi.org/10.1016/j.jog.2013.03.005

Vinci F., Iannace A., Parente M., Pirmez C., Torrieri S. & Giorgioni M. (2017) - *Early dolomitization in the Lower Cretaceous shallow-water carbonates of Southern Apennines (Italy): Clues about palaeoclimatic fluctuations in western Tethys.* Sedimentary Geology, **362**: 17-36. https://doi.org/10.1016/j.sedgeo.2017.10.007

Wang Z. & Bovik A.C. (2002) - *A universal image quality index*. IEEE Signal Processing Letters, **9**: 81-84. https://doi.org/10.1109/97.995823

Žabota B., Berger F. & Kobal M. (2023) - *The Potential of UAV-Acquired Photogrammetric and LiDAR-Point Clouds for Obtaining Rock Dimensions as Input Parameters for Modeling Rockfall Runout Zones.* Drones, **7**: 104. https://doi.org/10.3390/drones7020104

Zappaterra E. (1994) - *Source-Rock Distribution Model of the Periadriatic Region*. AAPG Bulletin, **78**: 333-354.

Zocchi M., Kasaragod A.K., Jenkins A., Cook C., Dobson R., Oommen T., Van Huis D., Taylor B., Brooks C., Marini R., Troiani F. & Mazzanti P. (2023) - *Multi-Sensor and Multi-Scale Remote Sensing Approach for Assessing Slope Instability along Transportation Corridors Using Satellites and Uncrewed Aircraft Systems.* Remote Sensing, **15**: 3016. https://doi.org/10.3390/rs15123016

Received November 2024 - Accepted December2024